Published in final edited form as:
Biol Psychiatry. 2015 March 15; 77(6): 556–568. doi:10.1016/j.biopsych.2014.06.026.

Pyramidal cell selective ablation of NMDA-R1 causes increase in cellular and network excitability

Valerie M. Tatard-Leitman, PhD[1,2], **Catherine R. Jutzeler**[1,2,†,‡], **Jimmy Suh**[1,2,†], **John A. Saunders, PhD**[1,2], **Eddie N. Billingslea, PhD**[1,2], **Susumu Morita**[1,#], **Rachel White, PhD**[2], **Robert E. Featherstone, PhD**[1,2], **Rabindranath Ray, PhD**[2], **Pavel I. Ortinski, PhD**[2], **Anamika Banerjee, PhD**[2], **Michael J. Gandal, PhD**[1], **Robert Lin**[1], **Anamaria Alexandrescu**[1], **Yuling Liang, MD**[1,2], **Raquel E. Gur, MD PhD**[2], **Karin E. Borgmann-Winter, MD**[2], **Gregory C. Carlson, PhD**[2], **Chang-Gyu Hahn, MD PhD**[2], and **Steven J. Siegel, MD PhD**[1,2]

[1]Translational Neuroscience Program, Department of Psychiatry, University of Pennsylvania, Philadelphia, PA 19104, USA

[2]Department of Psychiatry, University of Pennsylvania, Philadelphia, PA 19104, USA

Abstract

Background—Neuronal activity at gamma frequency is impaired in schizophrenia (SZ) and is considered critical for cognitive performance. Such impairments are thought to be due to reduced N-Methyl-D-Aspartate Receptor (NMDAR)-mediated inhibition from parvalbumin (PV) interneurons, rather than a direct role of impaired NMDAR signaling on pyramidal neurons. However, recent studies suggest a direct role of pyramidal neurons in regulating gamma oscillations. In particular, a computational model has been proposed in which phasic currents from pyramidal cells could drive synchronized feedback inhibition from interneurons. As such, impairments in pyramidal neuron activity could lead to abnormal gamma oscillations. However, this computational model has not been tested experimentally and the molecular mechanisms underlying pyramidal neuron dysfunction in SZ remain unclear.

Methods—In the present study, we tested the hypothesis that SZ-related phenotypes could arise from reduced NMDAR signaling in pyramidal neurons using forebrain pyramidal neurons specific NMDA-R1 knocked-out mice.

Correspondence should be addressed to: Steven J Siegel, Room 2202, Translational Research Laboratories, 125 S. 31st Street, University of Pennsylvania, Philadelphia, PA 19104, Phone: 215 573 0278, Fax: 215 573 2041, siegels@upenn.edu.
†Authors contributed equally to the study
‡Current address: University Clinic Balgrist, Zurich, Switzerland
#Current address: The University of Tokyo Faculty of Medicine, Tokyo, Japan

Financial Disclosures:
Steven Siegel reports grant support from Eli Lilly, AstraZeneca, NuPathe, and Pfizer that is unrelated to the content of this paper and consulting payments from Abbott, NuPathe, Merck, Sanofi, Boehringer Ingelheim and Wyeth that are unrelated to this work. The other authors report no biomedical financial interests or potential conflicts of interest.

Results—The mice displayed increased baseline gamma power as well as socio-cognitive impairments. These phenotypes were associated with increased pyramidal cell excitability due to changes in inherent membrane properties. Interestingly, mutant mice showed decreased expression of GIRK2 channels, which has been linked to increase neuronal excitability.

Conclusions—Our data demonstrate for the first time that NMDAR hypofunction in pyramidal cells is sufficient to cause electrophysiological, molecular, neuropathological and behavioral changes related to SZ.

Keywords

NMDA-R1; pyramidal neurons; hyperexcitability; Gamma frequency; GIRK; Schizophrenia

Introduction

Schizophrenia (SZ) is characterized by psychosis as well as profound social and cognitive impairments. EEG oscillatory activity at gamma frequencies (30–80Hz) is thought to reflect neural activity and functional connectivity that underlie social and cognitive function(1–3). Interestingly, abnormalities in gamma oscillations represent one of the most reproducible endophenotypes of SZ(4). Indeed, several studies have reported an increase in pre-stimulus gamma power in SZ patients during auditory paradigms(5, 6). A decrease in evoked gamma power has also been observed in SZ, when patients were exposed to simple auditory stimuli(7–14). Current studies have demonstrated that gamma oscillatory abnormalities can arise from excitatory-inhibitory (E/I) imbalance. E/I balance relies on reciprocal local-circuit connections among GABAergic interneurons and glutamatergic pyramidal neurons(15–17), for review(4, 18).

GABAergic interneurons expressing the calcium binding protein parvalbumin (PV) are particularly affected in SZ(19–21). Hypofunction of NMDAR signaling in these interneurons has been proposed to reduce feed forward inhibition, leading to abnormal gamma oscillations(1, 22). The resulting hyperexcitability has further been proposed as a mechanism for abnormal gamma oscillations in SZ, as well as SZ-related behavioral and cognitive impairments. A few recent studies using PV-specific NMDA-R1 knockout mice have reported enhanced baseline cortical gamma rhythms as well as impaired hippocampal synchrony. However, in these studies, the mutant mice showed largely normal behaviors except for selective cognitive impairments (*e.g.* deficits in habituation and working memory) (23, 24).

In a review published in 2012, Gonzales-Burgos and collaborators propose a new circuit model of inhibition-based gamma oscillations relevant to SZ, in which pyramidal neuron dysfunction could be the primary source of reduced interneuron activation(1). In this model, alterations in pyramidal neurons would lead to disrupted efferent drive onto interneurons, yielding abnormal synchronization of feedback inhibition. However, this model has not been tested experimentally and the mechanisms that would lead to dysfunction of the pyramidal neurons remain unknown.

NMDAR signaling is one of the major regulators of interneuron and pyramidal neuron excitability(22, 25). Preclinical and clinical studies focusing on pharmacology and genomics support the hypothesis that hypofunction of NMDAR signaling contributes to the pathophysiology of SZ(3, 26–31). For example, NMDA-R1 hypomorphic mice display SZ-like changes in oscillatory activity as well as social, cognitive and psychosis-related behaviors(32–38). Moreover, previous studies demonstrate that knocking out NMDA-R1 in pyramidal cells in hippocampal CA1 or CA3 induces a subset of cognitive deficits similar to those reported in SZ(39–41). However, the broader effect of knocking out NMDA-R1 in all forebrain pyramidal neurons has not been evaluated. Therefore, the present study was conducted to address this gap in understanding the potential mechanisms by which changes in NMDAR signaling specifically in pyramidal neurons may result in cellular, circuit-level and behavioral changes relevant to SZ.

Methods

Breeding strategy

Mice bearing a floxed NMDA-R1 allele were crossed with transgenic Camk2αCre mice, in which the expression of cre recombinase is driven in postmitotic pyramidal neurons(42). For more details see supplementary methods.

RNA and Protein Analysis

Tissues were surgically removed and were used either for In Situ Hybridization, Quantitative PCR or post-synaptic density fractionation(43) as detailed in supplementary methods.

Behavioral measures

All tests were performed blind to the genotypes of the subjects.

Social Interaction—Social behavior was assessed as described previously by Sankoorikal et *al.*(44). Social approach of test mice was measured toward same sex gonadectomized DBA/2J stimulus mice to minimize aggressive and sexual motivations of the test mouse. Test and stimulus mice were brought to the testing room in their home cages for a habituation period of approximately 30 min before starting the test. All behavioral tests were run in red light and videotaped. Further details are noted in supplemental methods.

Self-care behaviors—Assessment of nest building was performed as previously described(45). Further details are noted in supplemental methods.

Cognitive measures—Spatial working memory was assessed using both a continuous and discrete T-maze paradigm(46). Further details are noted in supplemental methods.

Open Field—Animals were tested in the open field as previously described(38). Further details are noted in supplemental methods.

Ex Vivo Electrophysiology

Mice aged 3–5 months were decapitated following isoflurane anesthesia. Further details are noted in supplemental methods.

In Vivo Electrophysiology

Animals were anesthetized with isoflurane and underwent stereotaxic implantation of tripolar electrode assemblies (PlasticsOne, Roanoke, VA, USA). EEG recording was performed at least a week after surgery on awake animals, in a home cage environment as previously described(36, 47–49) and see supplementary materials and methods. Baseline and auditory-evoked electrophysiological signals were recorded following paired-click stimuli using low-impedance macroelectrodes placed in hippocampal CA3 and the ipsilateral frontal sinus (positive electrode: 1.8 mm posterior, 2.65 mm right lateral, and 2.75 mm deep relative to Bregma). This differential recording configuration captures both early and late components of the auditoryevoked potential, including the acoustic brainstem response, mid-latency P20 (human P50/M50) and N40 (human N100/M100), as well as the late P2 and P3a peaks(50–52), with strong analogy to human scalp electroencephalogram (EEG)(47, 53).

Statistical Analysis

Statistical analyses were performed using Prism 5 software. Outliers were determined using Grubbs' test. Unpaired, two tailed t-test with Welch's correction or repeated measures ANOVA, with post-hoc Bonferroni were performed where appropriate as specified in figure legends. For nest building, quantitative PCR and western blot experiments the Mann Whitney U test was applied. (* - $p<0.05$, ** - $p<0.01$, *** - $p<0.001$). All data were Bonferroni corrected as follow: For behavioral experiments 4 measures were used $p=0.0125$ (social interaction, nest building, LMA, and T-maze); for EEG experiments, 9 measures were used $p=0.006$ (baseline activity, evoked activity, inter trial coherence at both gamma, theta and beta frequencies) and for patch clamp experiments 7 measures were used $p=0.007$ (frequency/current, RMP, sEPSC amplitude, sEPSC frequency, evoked EPSC, membrane resistance and rheobase). For QPCR experiments the data were corrected individually for each brain region (Hippocampus, Cortex and Striatum) and each group of markers (interneuron markers, dopamine receptors, serotonine receptors and AMPA-receptors).

Results

Characterization of pyramidal neuron specific NMDA-R1 knockout mice

We performed GAD67 immunostaining in transgenic Camk2αCre;(td)TomatoFlox mice in which the expression of the red fluorescent protein (td)Tomato is restricted to Camk2αCre expressing cells. No GAD67 co-staining was observed in (td)Tomato positive cells, demonstrating that no recombination occurred in GABAergic interneurons (Sup Fig. 1). We also showed that NMDA-R1 mRNA was decreased in most forebrain pyramidal neurons of the Camk2αCre-cKO mouse brains, except for a small population of cells in CA3 (Fig. 1A). The total expression was decreased by 57% in cortex ($p=0.006$), 66% in hippocampus ($p=0.006$) and 34% in striatum ($p=0.128$)(Fig. 1B). Moreover, whole-cell recordings in

hippocampal slices *in vitro* demonstrated the loss of NMDAR currents specifically in pyramidal cells of the Camk2αCre-cKO;(td)TomatoFlox compare to their wild type littermate Camk2αCre-WT;(td)TomatoFlox, while the AMPA currents where maintained in both genotypes ($p<0.005$)(Fig. 1C). We also confirmed the functional loss of NMDA-R1 in pyramidal neurons by measuring long-term potentiation (LTP) of field excitatory post-synaptic potentials (fEPSPs). When LTP was induced by tetanic stimuli, Camk2αCre-WT mice fEPSPs increased significantly from the baseline ($p=0.026$) and remained stable throughout the duration of recording ($p=0.002$). Conversely, Camk2αCre-cKO mice fEPSPs did not change significantly from baseline (Fig. 1D, E).

Loss of expression of NMDA-R1 in pyramidal neurons leads to SZ-like behavioral phenotypes

Social behavior was determined by assessing the time spent by the mice smelling the social and non-social cylinders. Camk2αCre-cKO mice spent significantly less time sniffing the social cylinder than Camk2αCre-WT mice ($p=0.008$)(Fig. 2A). Self-care was evaluated using a nest-building paradigm. Camk2αCre-cKO mice formed poor quality nests or no nest at all while the Camk2αCre-WT mice produced well-formed nests ($p<0.0001$)(Fig. 2B). LMA was assessed using automated software. Camk2αCre-cKO mice traveled approximately 1.78 times more than Camk2αCre-WT littermates ($p=0.002$)(Fig. 2C). Finally, we used both continuous and discrete T-Maze test tasks, as measures of working memory(46). For both tests, the Camk2αCre-cKO mice performed worse than the Camk2αCre-WT mice, showing a deficit in spatial working memory (Discrete T-maze: $p=0.028$; Continuous T-maze: $p=0.037$)(Fig. 2D).

Gamma, Theta and beta oscillatory activities were disturbed in pyramidal neuron specific NMDA-R1 KO mice

Gamma frequencies—We observed an increase in gamma EEG activity before (baseline/background) stimulus ($p<0.0001$)(Fig. 3A) and a decrease in stimulus evoked gamma activity ($p=0.006$)(Fig. 3B). These changes can also be represented as a decrease in the ratio of evoked to background activity ($p=0.001$). We also analyzed the inter-trial coherence (ITC) and did not observe a significant difference between the two groups of mice ($p=0.16$) (Fig. 3C).

Theta frequencies—We observed an increase of theta baseline activity in Camk2αCre-cKO mice ($p=0.002$)(Sup Fig. 2A) while theta evoked activity was reduced ($p=0.028$)(Sup Fig. 2B). As a result, the ratio of evoked to baseline activity was significantly decreased in the Camk2αCre-cKO compared to the Camk2αCre-WT mice ($p=0.015$). Finally, we observed a strong trend toward a decrease in ITC in the Camk2αCre-cKO mice, but the difference did not reach significance ($p=0.055$)(Sup Fig. 2C).

Beta frequencies—We observed an increase of beta baseline activity in Camk2αCre-cKO mice ($p=0.0001$)(Sup Fig. 3A) while beta evoked activity was reduced ($p=0.01$)(Sup Fig. 3B). As a result, the ratio of evoked to baseline activity was significantly decreased in the Camk2αCre-cKO compared to the Camk2αCre-WT mice ($p=0.0016$). Finally, we

observed a significant decrease in ITC in the Camk2αCre-cKO mice (p=0.022)(Sup Fig. 3C).

Loss of NMDA-R1 in pyramidal neurons leads to an increase in pyramidal cell excitability

Using patch clamp we found that pyramidal neurons in Camk2αCre-cKO mice fired significantly more action potentials in response to depolarizing current steps than neurons in the Camk2αCre-WT mice (p=0.001)(Fig. 4A). Accompanying this change we also observed an increase in the frequency/current slope (p=0.01)(Sup Fig. 4A), as well as a decrease in rheobase (p=0.028)(Sup Fig. 4B) in Camk2αCre-cKO mice compared to Camk2αCre-WT mice. Additionally, the resting membrane potential was significantly depolarized in Camk2αCre-cKO mice relative to the Camk2αCre-WT (p=0.007)(Fig. 4B). We also observed differences in synaptic properties between the two genotypes. Spontaneous EPSC (sEPSC) frequency was increased in the Camk2αCre-cKO mice (p=0.007)(Fig. 4C). Data indicate that there is an alteration of inherent membrane properties within pyramidal neurons in Camk2αCre-cKO mice, resulting in increased pyramidal cell excitability. However, the amplitude of sEPSC did not differ between the 2 groups (p=0.41)(Fig. 4D), suggesting that ion flux through individual channels was not different. Additionally, there was no difference in evoked EPSC between the two groups of mice (p=0.85) (Sup Fig. 4C), again suggesting that the primary alteration in network dynamics is due to changes in basal activity. Finally, no difference in membrane resistance was observed between the wild type and the transgenic mice (p=0.66)(Sup Fig. 4D).

Consequences of forebrain pyramidal neurons specific NMDA-R1 knock out on molecular markers relevant to SZ

Impact on GIRK channels and $GABA_{B2}$ receptors—We found a significant decrease of GIRK2 channel protein expression in the cortical synaptic membrane of Camk2αCre-cKO mice compared to Camk2αCre-WT mice (p=0.015)(Sup Fig. 5A). We also quantified $GABA_{B2}$ expression and phosphorylation at serine 783, which is a marker of receptor activation, in the cortical PSD. We did not observe any difference in the expression of $GABA_{B2}$ (data not shown, p=0.445) or in its level of activation P-$GABA_{B2}$/$GABA_{B2}$ (p=0.456)(Sup Fig. 5B).

Impact on dopaminergic and serotoninergic systems—In the cortex of Camk2αCre-cKO mice, we observed a significant decrease of the expression of DRD2 receptors (p=0.015)(Sup Fig. 6A) as well as a qualitative decrease of the expression of DRD1 (p=0.07)(Sup Fig. 6B). We also measured the expression of DRD1 and DRD2 mRNA in the hippocampus and the striatum and did not observe any difference between the two groups of mice (Sup Fig. 6A and B). Finally, there was no difference in the expression of the serotonin receptors 5HT1A, 5HT2A-B-C in the cortex, hippocampus or striatum, except for 5HT2A receptor, which was decreased in the hippocampus (p=0.008)(Sup Fig. 6C).

Impact on GABAergic system—We measured the level of expression of GAD67 mRNA in the cortex and hippocampus of the Camk2αCre-cKO and WT mice (Fig. 5A). We did not find any significant difference in expression between the two groups of mice

(Cortex: p=0.053; Hip: p=0.165). We did not find any changes in expression of PV mRNA in the Camk2αCre-cKO mice (Cortex: p=0.421; Hip: p=0.548)(Fig. 5B). However, we observed a decrease of CCK expression in the cortex of the Camk2αCre-cKO mice compared to Camk2αCre-WT mice (p=0.017)(Fig. 5C). No difference was observed in the hippocampus (p=0.151). Finally, we found a non-significant increase in somatostatin mRNA expression in the cortex and a qualitative increase in the hippocampus of the Camk2αCre-cKO mice (Cortex: p=0.056; Hip: p=0.259)(Fig. 5D).

Impact on AMPA receptors—We quantified the mRNA expression of GluR1–4 in the cortex and hippocampus and did not find any significant changes between the Camk2αCre-cKO mice and their wild type littermates (Cortex: GluR1 p=0.805; GluR2 p=0.180; GluR3 p=0.165; GluR4 p=0.456; Hippocampus: GluR1 p=0.456; GluR2 p=0.259; GluR3 p=0.945; GluR4 p=0.620)(Sup Fig. 7).

Discussion

Several studies of the role of NMDA-R1 knock out in GABAergic interneurons in relation with SZ have been reported. However, to date, none has focused on the role of the receptor specifically in pyramidal neurons. While there is limited data showing alteration of pyramidal neurons in SZ, post mortem studies have reported that SZ patients have abnormal pyramidal neurons with smaller soma, as well as abnormal laminar distribution and dendritic extensions(54, 55). Additionally, while no post mortem studies have reported a decrease of NMDA receptors expression in pyramidal cell in SZ patients, we have previously reported attenuated ligand-induced activation of NMDAR signaling in the post-mortem dorsolateral prefrontal cortex (DLPFC) of subjects with SZ compared to their matched controls(56). These data demonstrate a striking decrease in NMDA receptor function in the DLPFC of SZ cases compared to controls(56). The assessment of NMDA receptor function in this study was based on tissues homogenates. Thus the results do not distinguish between decreases in specific cell types. However, given that pyramidal neurons comprise up to 80 percent of the DLPFC and the DLPFC of SZ cases have shown striking decreases in NMDA receptor function, the data are consistent with primary dysfunction of pyramidal cells. Finally, previous animal studies demonstrate that knocking out NMDA-R1 in pyramidal cells restricted to hippocampal CA1 or CA3 induces a subset of cognitive deficits similar to those reported in SZ(39–41). Altogether, these studies highlight the importance of examining the broader effect of knocking out NMDA-R1 in all forebrain pyramidal neurons..

The Camk2α*C*re mice have been extensively used to knock out genes specifically in forebrain pyramidal excitatory neurons(57–62). While these studies have shown that recombination happens in pyramidal neurons, which we confirm here, no study has previously reported the absence of recombination in GABAergic interneurons. Because the aim of the present study was to demonstrate a role of NMDA-R1 restricted to excitatory cells in relation to SZ, it was important to confirm that the receptor was not knocked out in inhibitory interneurons. Using a cre reporter mouse line ((td)Tomato-Flox) we now demonstrate that the cre recombinase is not expressed in GABAergic GAD67 positive cells. To avoid possible down regulation of GAD67 expression caused by NMDA-R1 knock out, the mice used for this part of the study had not been crossed with NMDA-R1Flox mice. We

also report that there is no significant decrease in expression of NMDA-R1 in the striatum, where most neurons are GABAergic. Because we demonstrate here that no recombination occurs in GABAergic neurons, such decrease is most likely an indirect consequence of NMDA-R1 loss in pyramidal neurons. This result is interesting as striatal-specific manipulations can cause schizophrenia-like symptoms (63, 64). Finally, in the Camk2αCre mice used in this study the recombination starts at approximately 4 to 6 weeks of age, which is roughly equivalent to adolescence. Therefore, the changes that we report are occurring during the period that is similar to the prodromal period in SZ. As such, this model may be appropriate for alteration of NMDA receptor signaling that are manifest during adolescence and may precede the onset of the disease.

SZ is characterized by electrophysiological, behavioral and molecular disruption. We have performed a broad range of analysis covering these different areas in the pyramidal neuron specific NMDA-R1 knockout mice (Camk2αCre-cKO mice). Abnormalities in gamma oscillatory activity are among the most reproducible endophenotypes in SZ(4). Several studies have reported an increase in baseline activity(5, 6) and a decrease in evoked activity(7–14) in SZ patients. We found similar disruption in the Camk2αCre-cKO mice. These changes translated into a decrease in the ratio of evoked to background/baseline activity, which is consistent with the results obtained in previous clinical SZ studies(6, 65, 66). EEG oscillatory activity at gamma frequencies is thought to reflect neural activity underlying functional connectivity related to social and cognitive tasks processing. Accordingly, in the present study we observed impairment in social and cognitive behavior in the Camk2αCre-cKO mice. Several other behavioral impairments were also found in these mice such as a decrease in self-care and an increase locomotor activity. Locomotor activity is used as a measure of abnormal dopamine (DA) and serotonin (5-HT) functions, which are thought to be a major cause of psychosis(67, 68). We found a significant decrease of the expression of DRD2 receptors in the cortex of Camk2αCre-cKO mice but no significant changes occurred in the striatum. These results are in part in agreement with post mortem studies reporting a decrease of DRD2 expression in the forebrain and an increase in the striatum of patients with SZ(69–71) (and for review see(72, 73)).

The significant decrease in the ratio of evoked to background gamma activity in Camk2αCre-cKO mice may reflect a perturbation of E/I balance between GABAergic interneurons and pyramidal neurons in favor of increased excitability(38). We therefore examined cellular responses using current clamp in CA3 pyramidal cells. Altogether the patch clamp data converge toward an increase in pyramidal neuron and circuit excitability. Moreover, the data suggest that the primary alteration in network dynamics is due to changes in basal activity. We investigated possible mechanisms that could explain such phenotypes in the Camk2αCre-cKO mice.

Previous studies have demonstrated that NMDA-R1 activation increases the expression of GIRK channels, which facilitates hyperpolarization and reduces spike frequency under physiological condition(74, 75). Consequently, a decrease in GIRK channel activity would be in agreement with our results showing an increase in resting membrane potential as well as action potential firing frequency in the Camk2αCre-cKO. Interestingly, these mice did indeed have a decreased expression of GIRK2 in the synaptic membrane, where the majority

of GIRK channels reside. This result suggests that increased cellular and network excitability following NMDA-R1 knock out in pyramidal neurons could be in part explained by changes in GIRK channels expression and/or activity. Regulation of cellular excitability by GIRK channels depends on their level of expression, the activity of the channels and also their coupling with other proteins such as the $GABA_{B2}$ receptors(76–78). We did not find any difference in expression or activation the $GABA_{B2}$ receptors, suggesting that an alternative mechanism might be used to regulate the GIRK channels activity, such as direct regulation of GIRK currents.

The increase in pyramidal neuron and circuit excitability could also be explained by compensatory mechanisms through increased activity at non-NMDA glutamatergic receptors (i.e. AMPA and kainate receptors). Variability in AMPA-Receptors (GluRs) has been reported in post-mortem brain tissues from SZ patients. While most studies show a significant decrease in mRNA and protein expression(79–82), an increase in mRNA expression has also been reported(83). Moreover, it has been shown that knock out of NMDA-R1 in the hippocampus of mice leads to an enhancement of GluRs expression(84). Although the current study did not find any changes in expression of GluR1–4, we cannot rule out change in function. Indeed, Moghaddam and collaborators reported that the NMDAR antagonist ketamine results in increased stimulation of postsynaptic AMPA glutamate receptors(85). Future studies will determine if using non-NMDA glutamate receptor antagonists could help rescue the endophenotypes observed in the Camk2αCre-cKO mice.

Alterations of GABAergic interneurons have been repeatedly shown in SZ. Several post-mortem studies report a decrease in the expression of GAD67, the principal enzyme involved in GABA synthesis, in the prefrontal cortex and hippocampus of patients with SZ(19, 20, 86–91). However, we did not find a decrease in expression of GAD67 in Camk2αCre-cKO mice. A sub-population of GAD67 positive fast spiking GABAergic interneurons, positive for the calcium binding protein parvalbumin (PV), contributes to neural synchronization at gamma frequencies, and PV expression is consistently decreased in SZ. Moreover, it has been shown that ablation of NR1 in a subpopulation of GABAergic interneurons leads to a decrease in PV expression (92). We did not find any difference in PV mRNA expression between the Camk2αCre-cKO and their wild type littermates. This result could partly explain why we did not find any differences in gamma ITC. Moreover, it is possible that because we looked at the expression in the whole cortex, we obscured differences that would show up in a more restricted area such as the prefrontal cortex where changes of GAD67 and PV mRNA expression are the most often reported. In contrast to PV-interneurons, cholecystokinin (CCK) containing GABAergic interneurons are thought to be important in regulating EEG theta oscillations, and decreased CCK expression has also been reported in SZ(19, 93–95). Abnormalities in EEG measures at theta frequencies have been reported in SZ patients and in animal models of SZ(2, 47, 96–103). Additionally, theta modulation of gamma oscillatory activity is abnormal in SZ, and this disruption has been linked to altered NMDAR function in multiple animal and computational models(2, 3, 104"–106). Consistent with these results obtained in human and animal studies, we found a decrease in CCK mRNA expression as well as significant changes in EEG theta oscillations. Finally, in the hippocampus, somatostatin positive GABAergic interneurons play a key role

in gating network excitability(107–109) and somatostatin expression is decreased in post-mortem tissue of SZ patients, both in the hippocampus and prefrontal cortex(91, 110). However, we did not find any significant difference in somatostain mRNA expression in either the hippocampus or cortex of Camk2αCre-cKO mice. Altogether, our model reproduces some alterations in GABAergic interneurons that are reported in SZ. Future studies could determine the extent to which PV, CCK and somatostatin positive GABAergic interneurons display alterations in firing properties (EPSC and IPSCs) in the Camk2αCre-cKO mice.

In summary, the present study proposes an alternate mechanism to the prevailing disinhibition hypothesis, by which impairments in NMDAR signaling leads to symptoms and electrophysiological alterations related to SZ. Indeed, our results collectively provide direct evidence that reduced NMDA receptor signaling in pyramidal neurons can induce increased cellular and network excitability associated with SZ-like endophenotypes. Importantly, these data are consistent with the PING model that has been recently proposed by Gonzales-Burgos and collaborators in which pyramidal neuron dysfunction could be the primary source of reduced interneuron activation(1).

Supplementary Material

Refer to Web version on PubMed Central for supplementary material.

Acknowledgments

Funding: This work was supported by R01MH075916 (CGH), 5R01DA023210-02 (SJS), K01DA031747 (PIO), P50MH096891 (REG) and T32MH019112 (REG) as well as Developmental funds from the University of Pennsylvania (SJS).

References

1. Gonzalez-Burgos G, Lewis DA. NMDA Receptor Hypofunction, Parvalbumin-Positive Neurons and Cortical Gamma Oscillations in Schizophrenia. Schizophr Bull. 2012
2. Hamm JP, Gilmore CS, Picchetti NA, Sponheim SR, Clementz BA. Abnormalities of neuronal oscillations and temporal integration to low- and high-frequency auditory stimulation in schizophrenia. Biol Psychiatry. 2011; 69:989–996. [PubMed: 21216392]
3. Kirihara K, Rissling AJ, Swerdlow NR, Braff DL, Light GA. Hierarchical organization of gamma and theta oscillatory dynamics in schizophrenia. Biol Psychiatry. 2012; 71:873–880. [PubMed: 22361076]
4. Gandal MJ, Edgar JC, Klook K, Siegel SJ. Gamma synchrony: towards a translational biomarker for the treatment-resistant symptoms of schizophrenia. Neuropharmacology. 2012; 62:1504–1518. [PubMed: 21349276]
5. Hong LE, Summerfelt A, Mitchell BD, McMahon RP, Wonodi I, Buchanan RW, et al. Sensory gating endophenotype based on its neural oscillatory pattern and heritability estimate. Archives of general psychiatry. 2008; 65:1008–1016. [PubMed: 18762587]
6. Winterer G, Coppola R, Goldberg TE, Egan MF, Jones DW, Sanchez CE, et al. Prefrontal broadband noise, working memory, and genetic risk for schizophrenia. The American journal of psychiatry. 2004; 161:490–500. [PubMed: 14992975]
7. Basar-Eroglu C, Schmiedt-Fehr C, Mathes B, Zimmermann J, Brand A. Are oscillatory brain responses generally reduced in schizophrenia during long sustained attentional processing? International journal of psychophysiology : official journal of the International Organization of Psychophysiology. 2009; 71:75–83. [PubMed: 18725254]

8. Hall MH, Taylor G, Salisbury DF, Levy DL. Sensory gating event-related potentials and oscillations in schizophrenia patients and their unaffected relatives. Schizophrenia bulletin. 2011; 37:1187–1199. [PubMed: 20363872]

9. Hall MH, Taylor G, Sham P, Schulze K, Rijsdijk F, Picchioni M, et al. The early auditory gamma-band response is heritable and a putative endophenotype of schizophrenia. Schizophrenia bulletin. 2011; 37:778–787. [PubMed: 19946013]

10. Lee KH, Williams LM, Haig A, Goldberg E, Gordon E. An integration of 40 Hz Gamma and phasic arousal: novelty and routinization processing in schizophrenia. Clinical neurophysiology : official journal of the International Federation of Clinical Neurophysiology. 2001; 112:1499–1507. [PubMed: 11459690]

11. Leicht G, Karch S, Karamatskos E, Giegling I, Moller HJ, Hegerl U, et al. Alterations of the early auditory evoked gamma-band response in first-degree relatives of patients with schizophrenia: hints to a new intermediate phenotype. Journal of psychiatric research. 2011; 45:699–705. [PubMed: 21067772]

12. Leicht G, Kirsch V, Giegling I, Karch S, Hantschk I, Moller HJ, et al. Reduced early auditory evoked gamma-band response in patients with schizophrenia. Biological psychiatry. 2010; 67:224–231. [PubMed: 19765689]

13. Lenz D, Fischer S, Schadow J, Bogerts B, Herrmann CS. Altered evoked gamma-band responses as a neurophysiological marker of schizophrenia? International journal of psychophysiology : official journal of the International Organization of Psychophysiology. 2011; 79:25–31. [PubMed: 20705107]

14. Teale P, Collins D, Maharajh K, Rojas DC, Kronberg E, Reite M. Cortical source estimates of gamma band amplitude and phase are different in schizophrenia. NeuroImage. 2008; 42:1481–1489. [PubMed: 18634887]

15. Atallah BV, Scanziani M. Instantaneous modulation of gamma oscillation frequency by balancing excitation with inhibition. Neuron. 2009; 62:566–577. [PubMed: 19477157]

16. Economo MN, White JA. Membrane properties and the balance between excitation and inhibition control gamma-frequency oscillations arising from feedback inhibition. PLoS computational biology. 2012; 8:e1002354. [PubMed: 22275859]

17. Yizhar O, Fenno LE, Prigge M, Schneider F, Davidson TJ, O'Shea DJ, et al. Neocortical excitation/inhibition balance in information processing and social dysfunction. Nature. 2011; 477:171–178. [PubMed: 21796121]

18. Ford JM, Krystal JH, Mathalon DH. Neural synchrony in schizophrenia: from networks to new treatments. Schizophrenia bulletin. 2007; 33:848–852. [PubMed: 17567628]

19. Hashimoto T, Arion D, Unger T, Maldonado-Aviles JG, Morris HM, Volk DW, et al. Alterations in GABA-related transcriptome in the dorsolateral prefrontal cortex of subjects with schizophrenia. Mol Psychiatry. 2008; 13:147–161. [PubMed: 17471287]

20. Hashimoto T, Volk DW, Eggan SM, Mirnics K, Pierri JN, Sun Z, et al. Gene expression deficits in a subclass of GABA neurons in the prefrontal cortex of subjects with schizophrenia. J Neurosci. 2003; 23:6315–6326. [PubMed: 12867516]

21. Mellios N, Huang HS, Baker SP, Galdzicka M, Ginns E, Akbarian S. Molecular determinants of dysregulated GABAergic gene expression in the prefrontal cortex of subjects with schizophrenia. Biol Psychiatry. 2009; 65:1006–1014. [PubMed: 19121517]

22. Homayoun H, Moghaddam B. NMDA receptor hypofunction produces opposite effects on prefrontal cortex interneurons and pyramidal neurons. The Journal of neuroscience : the official journal of the Society for Neuroscience. 2007; 27:11496–11500. [PubMed: 17959792]

23. Korotkova T, Fuchs EC, Ponomarenko A, von Engelhardt J, Monyer H. NMDA receptor ablation on parvalbumin-positive interneurons impairs hippocampal synchrony, spatial representations, and working memory. Neuron. 2010; 68:557–569. [PubMed: 21040854]

24. Carlen M, Meletis K, Siegle JH, Cardin JA, Futai K, Vierling-Claassen D, et al. A critical role for NMDA receptors in parvalbumin interneurons for gamma rhythm induction and behavior. Mol Psychiatry. 2012; 17:537–548. [PubMed: 21468034]

25. Xue JG, Masuoka T, Gong XD, Chen KS, Yanagawa Y, Law SK, et al. NMDA receptor activation enhances inhibitory GABAergic transmission onto hippocampal pyramidal neurons via

presynaptic and postsynaptic mechanisms. Journal of neurophysiology. 2011; 105:2897–2906. [PubMed: 21471392]

26. Javitt DC, Zukin SR. Recent advances in the phencyclidine model of schizophrenia. The American journal of psychiatry. 1991; 148:1301–1308. [PubMed: 1654746]
27. Jentsch JD, Andrusiak E, Tran A, Bowers MB Jr, Roth RH. Delta 9-tetrahydrocannabinol increases prefrontal cortical catecholaminergic utilization and impairs spatial working memory in the rat: blockade of dopaminergic effects with HA966. Neuropsychopharmacology : official publication of the American College of Neuropsychopharmacology. 1997; 16:426–432. [PubMed: 9165498]
28. Krystal JH, Karper LP, Seibyl JP, Freeman GK, Delaney R, Bremner JD, et al. Subanesthetic effects of the noncompetitive NMDA antagonist, ketamine, in humans. Psychotomimetic, perceptual, cognitive, and neuroendocrine responses. Arch Gen Psychiatry. 1994; 51:199–214. [PubMed: 8122957]
29. Lahti AC, Koffel B, LaPorte D, Tamminga CA. Subanesthetic doses of ketamine stimulate psychosis in schizophrenia. Neuropsychopharmacology. 1995; 13:9–19. [PubMed: 8526975]
30. Lahti AC, Weiler MA, Tamara Michaelidis BA, Parwani A, Tamminga CA. Effects of ketamine in normal and schizophrenic volunteers. Neuropsychopharmacology : official publication of the American College of Neuropsychopharmacology. 2001; 25:455–467. [PubMed: 11557159]
31. Stone JM, Erlandsson K, Arstad E, Squassante L, Teneggi V, Bressan RA, et al. Relationship between ketamine-induced psychotic symptoms and NMDA receptor occupancy: a [(123)I]CNS-1261 SPET study. Psychopharmacology. 2008; 197:401–408. [PubMed: 18176855]
32. Bickel S, Lipp HP, Umbricht D. Impaired attentional modulation of auditory evoked potentials in N-methyl-D-aspartate NR1 hypomorphic mice. Genes Brain Behav. 2007; 6:558–568. [PubMed: 17116169]
33. Duncan G, Miyamoto S, Gu H, Lieberman J, Koller B, Snouwaert J. Alterations in regional brain metabolism in genetic and pharmacological models of reduced NMDA receptor function. Brain research. 2002; 951:166–176. [PubMed: 12270494]
34. Duncan GE, Moy SS, Perez A, Eddy DM, Zinzow WM, Lieberman JA, et al. Deficits in sensorimotor gating and tests of social behavior in a genetic model of reduced NMDA receptor function. Behavioural brain research. 2004; 153:507–519. [PubMed: 15265649]
35. Dzirasa K, Ramsey AJ, Takahashi DY, Stapleton J, Potes JM, Williams JK, et al. Hyperdopaminergia and NMDA receptor hypofunction disrupt neural phase signaling. The Journal of neuroscience : the official journal of the Society for Neuroscience. 2009; 29:8215–8224. [PubMed: 19553461]
36. Halene TB, Ehrlichman RS, Liang Y, Christian EP, Jonak GJ, Gur TL, et al. Assessment of NMDA receptor NR1 subunit hypofunction in mice as a model for schizophrenia. Genes Brain Behav. 2009; 8:661–675. [PubMed: 19563516]
37. Mohn AR, Gainetdinov RR, Caron MG, Koller BH. Mice with reduced NMDA receptor expression display behaviors related to schizophrenia. Cell. 1999; 98:427–436. [PubMed: 10481908]
38. Gandal MJ, Sisti J, Klook K, Ortinski PI, Leitman V, Liang Y, et al. GABAB-mediated rescue of altered excitatory-inhibitory balance, gamma synchrony and behavioral deficits following constitutive NMDAR-hypofunction. Translational psychiatry. 2012; 2:e142. [PubMed: 22806213]
39. Li C, Niu W, Jiang CH, Hu Y. Effects of enriched environment on gene expression and signal pathways in cortex of hippocampal CA1 specific NMDAR1 knockout mice. Brain Res Bull. 2007; 71:568–577. [PubMed: 17292799]
40. McHugh TJ, Blum KI, Tsien JZ, Tonegawa S, Wilson MA. Impaired hippocampal representation of space in CA1-specific NMDAR1 knockout mice. Cell. 1996; 87:1339–1349. [PubMed: 8980239]
41. Rampon C, Tang YP, Goodhouse J, Shimizu E, Kyin M, Tsien JZ. Enrichment induces structural changes and recovery from nonspatial memory deficits in CA1 NMDAR1-knockout mice. Nature neuroscience. 2000; 3:238–244.
42. Tsien JZ, Chen DF, Gerber D, Tom C, Mercer EH, Anderson DJ, et al. Subregion- and cell type-restricted gene knockout in mouse brain. Cell. 1996; 87:1317–1326. [PubMed: 8980237]

43. Wang HY, Friedman E. Enhanced protein kinase C activity and translocation in bipolar affective disorder brains. Biological psychiatry. 1996; 40:568–575. [PubMed: 8886289]
44. Sankoorikal GM, Kaercher KA, Boon CJ, Lee JK, Brodkin ES. A mouse model system for genetic analysis of sociability: C57BL/6J versus BALB/cJ inbred mouse strains. Biol Psychiatry. 2006; 59:415–423. [PubMed: 16199013]
45. Deacon RM. Assessing nest building in mice. Nat Protoc. 2006; 1:1117–1119. [PubMed: 17406392]
46. Deacon RM, Rawlins JN. T-maze alternation in the rodent. Nat Protoc. 2006; 1:7–12. [PubMed: 17406205]
47. Ehrlichman RS, Gandal MJ, Maxwell CR, Lazarewicz MT, Finkel LH, Contreras D, et al. N-methyl-d-aspartic acid receptor antagonist-induced frequency oscillations in mice recreate pattern of electrophysiological deficits in schizophrenia. Neuroscience. 2009; 158:705–712. [PubMed: 19015010]
48. Gandal MJ, Ehrlichman RS, Rudnick ND, Siegel SJ. A novel electrophysiological model of chemotherapy-induced cognitive impairments in mice. Neuroscience. 2008; 157:95–104. [PubMed: 18835334]
49. Lazarewicz MT, Ehrlichman RS, Maxwell CR, Gandal MJ, Finkel LH, Siegel SJ. Ketamine modulates theta and gamma oscillations. J Cogn Neurosci. 2010; 22:1452–1464. [PubMed: 19583475]
50. Connolly PM, Maxwell C, Liang Y, Kahn JB, Kanes SJ, Abel T, et al. The effects of ketamine vary among inbred mouse strains and mimic schizophrenia for the P80, but not P20 or N40 auditory ERP components. Neurochemical research. 2004; 29:1179–1188. [PubMed: 15176475]
51. Connolly PM, Maxwell CR, Kanes SJ, Abel T, Liang Y, Tokarczyk J, et al. Inhibition of auditory evoked potentials and prepulse inhibition of startle in DBA/2J and DBA/2Hsd inbred mouse substrains. Brain research. 2003; 992:85–95. [PubMed: 14604776]
52. Siegel SJ, Connolly P, Liang Y, Lenox RH, Gur RE, Bilker WB, et al. Effects of strain, novelty, and NMDA blockade on auditory-evoked potentials in mice. Neuropsychopharmacology : official publication of the American College of Neuropsychopharmacology. 2003; 28:675–682. [PubMed: 12655312]
53. Gandal MJ, Edgar JC, Ehrlichman RS, Mehta M, Roberts TP, Siegel SJ. Validating gamma oscillations and delayed auditory responses as translational biomarkers of autism. Biol Psychiatry. 2010; 68:1100–1106. [PubMed: 21130222]
54. Arnold SE, Hyman BT, Van Hoesen GW, Damasio AR. Some cytoarchitectural abnormalities of the entorhinal cortex in schizophrenia. Arch Gen Psychiatry. 1991; 48:625–632. [PubMed: 2069493]
55. Arnold SE, Ruscheinsky DD, Han LY. Further evidence of abnormal cytoarchitecture of the entorhinal cortex in schizophrenia using spatial point pattern analyses. Biol Psychiatry. 1997; 42:639–647. [PubMed: 9325556]
56. Hahn CG, Wang HY, Cho DS, Talbot K, Gur RE, Berrettini WH, et al. Altered neuregulin 1-erbB4 signaling contributes to NMDA receptor hypofunction in schizophrenia. Nat Med. 2006; 12:824–828. [PubMed: 16767099]
57. Feng R, Wang H, Wang J, Shrom D, Zeng X, Tsien JZ. Forebrain degeneration and ventricle enlargement caused by double knockout of Alzheimer's presenilin-1 and presenilin-2. Proceedings of the National Academy of Sciences of the United States of America. 2004; 101:8162–8167. [PubMed: 15148382]
58. Ferguson C, Hardy SL, Werner DF, Hileman SM, Delorey TM, Homanics GE. New insight into the role of the beta3 subunit of the GABAA-R in development, behavior, body weight regulation, and anesthesia revealed by conditional gene knockout. BMC neuroscience. 2007; 8:85. [PubMed: 17927825]
59. Kiselycznyk C, Svenningsson P, Delpire E, Holmes A. Genetic, pharmacological and lesion analyses reveal a selective role for corticohippocampal GLUN2B in a novel repeated swim stress paradigm. Neuroscience. 2011; 193:259–268. [PubMed: 21704131]

60. Mirnics K, Norstrom EM, Garbett K, Choi SH, Zhang X, Ebert P, et al. Molecular signatures of neurodegeneration in the cortex of PS1/PS2 double knockout mice. Molecular neurodegeneration. 2008; 3:14. [PubMed: 18834536]

61. Sato C, Turkoz M, Dearborn JT, Wozniak DF, Kopan R, Hass MR. Loss of RBPj in postnatal excitatory neurons does not cause neurodegeneration or memory impairments in aged mice. PloS one. 2012; 7:e48180. [PubMed: 23110206]

62. Valor LM, Pulopulos MM, Jimenez-Minchan M, Olivares R, Lutz B, Barco A. Ablation of CBP in forebrain principal neurons causes modest memory and transcriptional defects and a dramatic reduction of histone acetylation but does not affect cell viability. The Journal of neuroscience : the official journal of the Society for Neuroscience. 2011; 31:1652–1663. [PubMed: 21289174]

63. Kellendonk C. Modeling excess striatal D2 receptors in mice. Progress in brain research. 2009; 179:59–65. [PubMed: 20302818]

64. Kellendonk C, Simpson EH, Polan HJ, Malleret G, Vronskaya S, Winiger V, et al. Transient and selective overexpression of dopamine D2 receptors in the striatum causes persistent abnormalities in prefrontal cortex functioning. Neuron. 2006; 49:603–615. [PubMed: 16476668]

65. Krishnan GP, Vohs JL, Hetrick WP, Carroll CA, Shekhar A, Bockbrader MA, et al. Steady state visual evoked potential abnormalities in schizophrenia. Clinical neurophysiology : official journal of the International Federation of Clinical Neurophysiology. 2005; 116:614–624. [PubMed: 15721075]

66. Winterer G, Ziller M, Dorn H, Frick K, Mulert C, Wuebben Y, et al. Schizophrenia: reduced signal-to-noise ratio and impaired phase-locking during information processing. Clinical neurophysiology : official journal of the International Federation of Clinical Neurophysiology. 2000; 111:837–849. [PubMed: 10802455]

67. Burnet PW, Eastwood SL, Harrison PJ. 5-HT1A and 5-HT2A receptor mRNAs and binding site densities are differentially altered in schizophrenia. Neuropsychopharmacology. 1996; 15:442–455. [PubMed: 8914117]

68. Knable MB, Barci BM, Bartko JJ, Webster MJ, Torrey EF. Molecular abnormalities in the major psychiatric illnesses: Classification and Regression Tree (CRT) analysis of post-mortem prefrontal markers. Mol Psychiatry. 2002; 7:392–404. [PubMed: 11986983]

69. Seeman P, Bzowej NH, Guan HC, Bergeron C, Reynolds GP, Bird ED, et al. Human brain D1 and D2 dopamine receptors in schizophrenia, Alzheimer's, Parkinson's, and Huntington's diseases. Neuropsychopharmacology : official publication of the American College of Neuropsychopharmacology. 1987; 1:5–15. [PubMed: 2908095]

70. Suhara T, Okubo Y, Yasuno F, Sudo Y, Inoue M, Ichimiya T, et al. Decreased dopamine D2 receptor binding in the anterior cingulate cortex in schizophrenia. Archives of general psychiatry. 2002; 59:25–30. [PubMed: 11779278]

71. Tuppurainen H, Kuikka J, Viinamaki H, Husso-Saastamoinen M, Bergstrom K, Tiihonen J. Extrastriatal dopamine D 2/3 receptor density and distribution in drug-naive schizophrenic patients. Molecular psychiatry. 2003; 8:453–455. [PubMed: 12740603]

72. Howes OD, Kapur S. The dopamine hypothesis of schizophrenia: version III--the final common pathway. Schizophrenia bulletin. 2009; 35:549–562. [PubMed: 19325164]

73. Takahashi H, Higuchi M, Suhara T. The role of extrastriatal dopamine D2 receptors in schizophrenia. Biological psychiatry. 2006; 59:919–928. [PubMed: 16682269]

74. Chung HJ, Ge WP, Qian X, Wiser O, Jan YN, Jan LY. G protein-activated inwardly rectifying potassium channels mediate depotentiation of long-term potentiation. Proceedings of the National Academy of Sciences of the United States of America. 2009; 106:635–640. [PubMed: 19118199]

75. Chung HJ, Qian X, Ehlers M, Jan YN, Jan LY. Neuronal activity regulates phosphorylation-dependent surface delivery of G protein-activated inwardly rectifying potassium channels. Proceedings of the National Academy of Sciences of the United States of America. 2009; 106:629–634. [PubMed: 19118198]

76. Labouebe G, Lomazzi M, Cruz HG, Creton C, Lujan R, Li M, et al. RGS2 modulates coupling between GABAB receptors and GIRK channels in dopamine neurons of the ventral tegmental area. Nature neuroscience. 2007; 10:1559–1568.

77. Padgett CL, Slesinger PA. GABAB receptor coupling to G-proteins and ion channels. Adv Pharmacol. 2010; 58:123–147. [PubMed: 20655481]

78. Xie K, Allen KL, Kourrich S, Colon-Saez J, Thomas MJ, Wickman K, et al. Gbeta5 recruits R7 RGS proteins to GIRK channels to regulate the timing of neuronal inhibitory signaling. Nat Neurosci. 2010; 13:661–663. [PubMed: 20453851]

79. Beneyto M, Meador-Woodruff JH. Lamina-specific abnormalities of AMPA receptor trafficking and signaling molecule transcripts in the prefrontal cortex in schizophrenia. Synapse. 2006; 60:585–598. [PubMed: 16983646]

80. Breese CR, Freedman R, Leonard SS. Glutamate receptor subtype expression in human postmortem brain tissue from schizophrenics and alcohol abusers. Brain research. 1995; 674:82–90. [PubMed: 7773698]

81. Corti C, Xuereb JH, Crepaldi L, Corsi M, Michielin F, Ferraguti F. Altered levels of glutamatergic receptors and Na+/K+ ATPase-alpha1 in the prefrontal cortex of subjects with schizophrenia. Schizophrenia research. 2011; 128:7–14. [PubMed: 21353485]

82. Eastwood SL, McDonald B, Burnet PW, Beckwith JP, Kerwin RW, Harrison PJ. Decreased expression of mRNAs encoding non-NMDA glutamate receptors GluR1 and GluR2 in medial temporal lobe neurons in schizophrenia. Brain research Molecular brain research. 1995; 29:211–223. [PubMed: 7609609]

83. Dracheva S, McGurk SR, Haroutunian V. mRNA expression of AMPA receptors and AMPA receptor binding proteins in the cerebral cortex of elderly schizophrenics. Journal of neuroscience research. 2005; 79:868–878. [PubMed: 15696539]

84. Lu W, Gray JA, Granger AJ, During MJ, Nicoll RA. Potentiation of synaptic AMPA receptors induced by the deletion of NMDA receptors requires the GluA2 subunit. Journal of neurophysiology. 2011; 105:923–928. [PubMed: 20980546]

85. Moghaddam B, Adams B, Verma A, Daly D. Activation of glutamatergic neurotransmission by ketamine: a novel step in the pathway from NMDA receptor blockade to dopaminergic and cognitive disruptions associated with the prefrontal cortex. J Neurosci. 1997; 17:2921–2927. [PubMed: 9092613]

86. Curley AA, Arion D, Volk DW, Asafu-Adjei JK, Sampson AR, Fish KN, et al. Cortical deficits of glutamic acid decarboxylase 67 expression in schizophrenia: clinical, protein, and cell type-specific features. The American journal of psychiatry. 2011; 168:921–929. [PubMed: 21632647]

87. Duncan CE, Webster MJ, Rothmond DA, Bahn S, Elashoff M, Shannon Weickert C. Prefrontal GABA(A) receptor alpha-subunit expression in normal postnatal human development and schizophrenia. Journal of psychiatric research. 2010; 44:673–681. [PubMed: 20100621]

88. Torrey EF, Barci BM, Webster MJ, Bartko JJ, Meador-Woodruff JH, Knable MB. Neurochemical markers for schizophrenia, bipolar disorder, and major depression in postmortem brains. Biological psychiatry. 2005; 57:252–260. [PubMed: 15691526]

89. Volk DW, Matsubara T, Li S, Sengupta EJ, Georgiev D, Minabe Y, et al. Deficits in transcriptional regulators of cortical parvalbumin neurons in schizophrenia. The American journal of psychiatry. 2012; 169:1082–1091. [PubMed: 22983435]

90. Woo TU, Kim AM, Viscidi E. Disease-specific alterations in glutamatergic neurotransmission on inhibitory interneurons in the prefrontal cortex in schizophrenia. Brain research. 2008; 1218:267–277. [PubMed: 18534564]

91. Konradi C, Yang CK, Zimmerman EI, Lohmann KM, Gresch P, Pantazopoulos H, et al. Hippocampal interneurons are abnormal in schizophrenia. Schizophrenia research. 2011; 131:165–173. [PubMed: 21745723]

92. Belforte JE, Zsiros V, Sklar ER, Jiang Z, Yu G, Li Y, et al. Postnatal NMDA receptor ablation in corticolimbic interneurons confers schizophrenia-like phenotypes. Nature neuroscience. 2010; 13:76–83.

93. Fung SJ, Webster MJ, Sivagnanasundaram S, Duncan C, Elashoff M, Weickert CS. Expression of interneuron markers in the dorsolateral prefrontal cortex of the developing human and in schizophrenia. Am J Psychiatry. 2010; 167:1479–1488. [PubMed: 21041246]

94. Klausberger T, Marton LF, O'Neill J, Huck JH, Dalezios Y, Fuentealba P, et al. Complementary roles of cholecystokinin- and parvalbumin-expressing GABAergic neurons in hippocampal network oscillations. J Neurosci. 2005; 25:9782–9793. [PubMed: 16237182]

95. Klausberger T, Somogyi P. Neuronal diversity and temporal dynamics: the unity of hippocampal circuit operations. Science. 2008; 321:53–57. [PubMed: 18599766]

96. Basar-Eroglu C, Schmiedt-Fehr C, Marbach S, Brand A, Mathes B. Altered oscillatory alpha and theta networks in schizophrenia. Brain research. 2008; 1235:143–152. [PubMed: 18657525]

97. Bates AT, Kiehl KA, Laurens KR, Liddle PF. Low-frequency EEG oscillations associated with information processing in schizophrenia. Schizophrenia research. 2009; 115:222–230. [PubMed: 19850450]

98. Doege K, Bates AT, White TP, Das D, Boks MP, Liddle PF. Reduced event-related low frequency EEG activity in schizophrenia during an auditory oddball task. Psychophysiology. 2009; 46:566–577. [PubMed: 19298628]

99. Donkers FC, Schwikert SR, Evans AM, Cleary KM, Perkins DO, Belger A. Impaired neural synchrony in the theta frequency range in adolescents at familial risk for schizophrenia. Frontiers in psychiatry / Frontiers Research Foundation. 2011; 2:51.

100. Hong LE, Summerfelt A, Mitchell BD, O'Donnell P, Thaker GK. A shared low-frequency oscillatory rhythm abnormality in resting and sensory gating in schizophrenia. Clinical neurophysiology : official journal of the International Federation of Clinical Neurophysiology. 2012; 123:285–292. [PubMed: 21862398]

101. Kittelberger K, Hur EE, Sazegar S, Keshavan V, Kocsis B. Comparison of the effects of acute and chronic administration of ketamine on hippocampal oscillations: relevance for the NMDA receptor hypofunction model of schizophrenia. Brain structure & function. 2012; 217:395–409. [PubMed: 21979451]

102. Schmiedt C, Brand A, Hildebrandt H, Basar-Eroglu C. Event-related theta oscillations during working memory tasks in patients with schizophrenia and healthy controls. Brain research Cognitive brain research. 2005; 25:936–947. [PubMed: 16289526]

103. Westphal KP, Grozinger B, Diekmann V, Scherb W, Reess J, Leibing U, et al. Slower theta activity over the midfrontal cortex in schizophrenic patients. Acta psychiatrica Scandinavica. 1990; 81:132–138. [PubMed: 2327275]

104. Dickerson DD, Wolff AR, Bilkey DK. Abnormal long-range neural synchrony in a maternal immune activation animal model of schizophrenia. J Neurosci. 2010; 30:12424–12431. [PubMed: 20844137]

105. Neymotin SA, Lazarewicz MT, Sherif M, Contreras D, Finkel LH, Lytton WW. Ketamine disrupts theta modulation of gamma in a computer model of hippocampus. J Neurosci. 2011; 31:11733–11743. [PubMed: 21832203]

106. Wolf JA, Moyer JT, Lazarewicz MT, Contreras D, Benoit-Marand M, O'Donnell P, et al. NMDA/AMPA ratio impacts state transitions and entrainment to oscillations in a computational model of the nucleus accumbens medium spiny projection neuron. J Neurosci. 2005; 25:9080–9095. [PubMed: 16207867]

107. Greene JR, Mason A. Neuronal diversity in the subiculum: correlations with the effects of somatostatin on intrinsic properties and on GABA-mediated IPSPs in vitro. Journal of neurophysiology. 1996; 76:1657–1666. [PubMed: 8890283]

108. Greene JR, Mason A. Effects of somatostatin and related peptides on the membrane potential and input resistance of rat ventral subicular neurons, in vitro. The Journal of pharmacology and experimental therapeutics. 1996; 276:426–432. [PubMed: 8632306]

109. Schweitzer P, Madamba SG, Siggins GR. Somatostatin increases a voltage-insensitive K+ conductance in rat CA1 hippocampal neurons. Journal of neurophysiology. 1998; 79:1230–1238. [PubMed: 9497404]

110. Morris HM, Hashimoto T, Lewis DA. Alterations in somatostatin mRNA expression in the dorsolateral prefrontal cortex of subjects with schizophrenia or schizoaffective disorder. Cereb Cortex. 2008; 18:1575–1587. [PubMed: 18203698]

111. Roach BJ, Mathalon DH. Event-related EEG time-frequency analysis: an overview of measures and an analysis of early gamma band phase locking in schizophrenia. Schizophrenia bulletin. 2008; 34:907–926. [PubMed: 18684772]

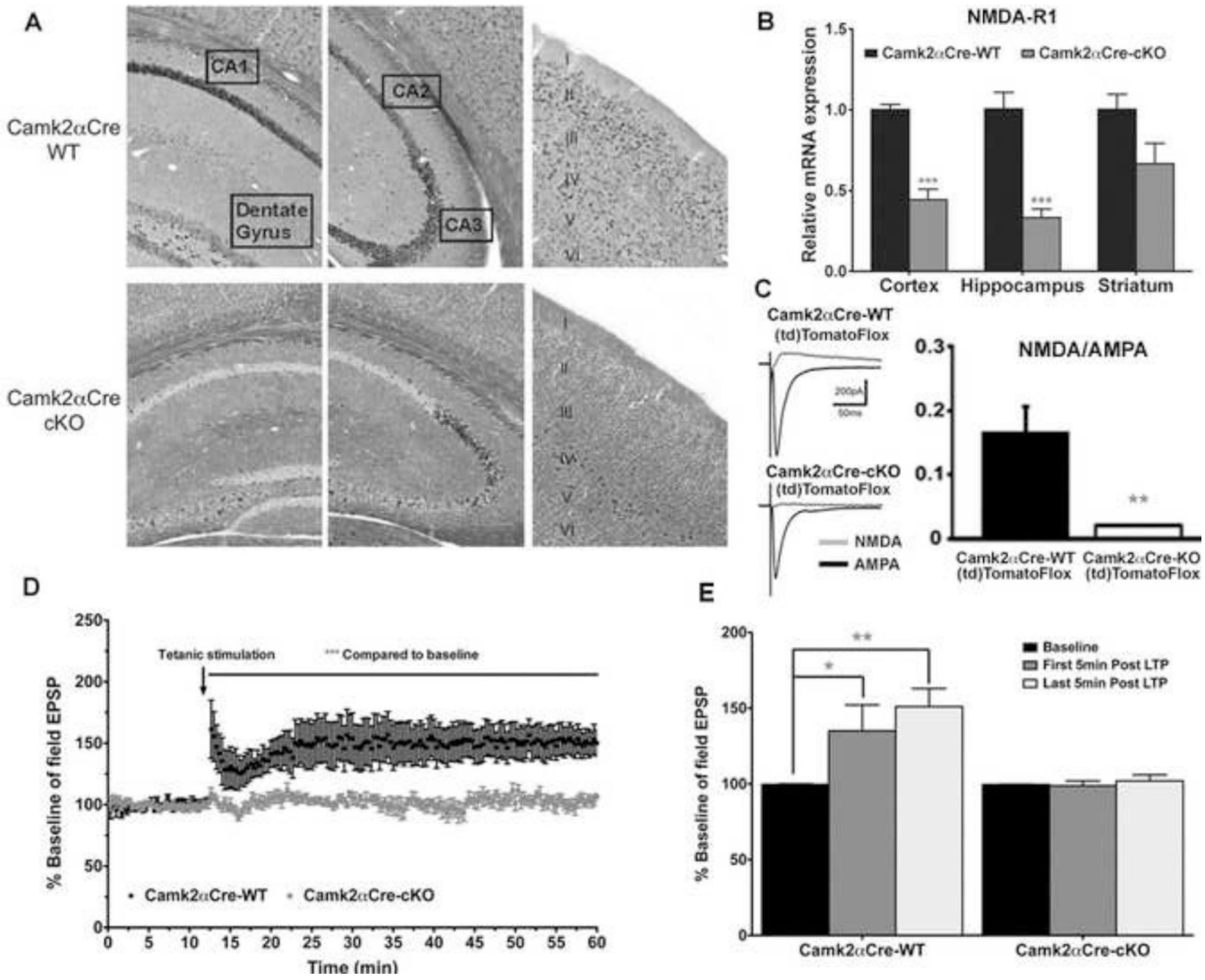

Figure 1. Pyramidal neuron specific NMDA-R1 KO characterization

A) *In Situ* Hybridization showing the localization of NMDA-R1 mRNA in Camk2αCre-WT (top panel) and Camk2αCre-cKO (bottom panel) mice. Left panel: expression in the CA1 and dentate gyrus, Middle panel: expression in CA2 and CA3 and Right panel: expression in the neocortex, layers I through VI. Note that the expression of NMDA-R1 mRNA was reduced in all layers of neocortex in CamkαCre-cKO mice, except layer IV where interneurons are positioned. NMDA-R1 mRNA expression was also lost throughout CA1, CA2 and the dentate gyrus, while scattered expression remains in CA3. **B)** Real-time PCR quantification of NMDA-R1 mRNA, in the cortex, hippocampus, and striatum of the Camk2αCre-cKO and Camk2αCre-WT mice. The expression in the Camk2αCre-cKO mice is normalized to the expression in the Camk2αCre-WT mice. The expression of NMDA-R1 mRNA is significantly decreased by 66% in the hippocampus and 57% in the cortex, while a non-significant decrease is observed in the striatum (Cortex: Camk2αCre-WT=1±0.04, n=7; Camk2αCre-cKO=0.44±0.07, n=7; p=0.0006. Hippocampus: Camk2αCre-WT=1±0.01, n=7; Camk2αCre-cKO=0.34±0.05, n=7; p=0.0006. Striatum: Camk2αCre-WT=1±0.09,

n=7; Cam2aCre-cKO=0.67±0.13, n=7; p=0.1282, Mann-Withney, two tailed, all samples were run in duplicate). **C)** Whole-cell recordings in hippocampal slices *in vitro*. NMDA currents in pyramidal cells are lost while AMPA currents are preserved. (Camk2αCre-WT; (td)TomatoFlox: NMDA/AMPA ratio=0.16±0.04, n=6 cells/4 mice; Camk2αCre-cKO; (td)TomatoFlox, NMDA/AMPA ratio=0.02±0.001, 6 cells/3 mice, p<0.005, unpaired t-test). **D, E)** NMDA-R1 loss in pyramidal neurons prevents long-term potentiation. Field excitatory post-synaptic potentials (fEPSPs) were recorded in the CA1 area of the hippocampus at baseline (first 15 minutes) and following the 2 tetanic stimuli (During 45 minutes) in CA1. Note the complete absence of LTP in the Camk2αCre-cKO mice. **D)** Following the tetanic stimuli, Camk2αCre-WT mice developed long-term potentiation, which lasted for over one hour. However, Camk2αCre-cKO mice did not develop LTP, as the fEPSPs were not different before and after the tetanic stimuli. (Camk2αCre-WT: Baseline fEPSPs=99.69±0.25 %, All fEPSPs after tetanic stimuli=147.66±13.40 %, n=6; p=0.0048; Camk2αCre-cKO: Baseline fEPSPs=99.62±0.17 %, All fEPSPs after tetanic stimuli=102.07±2.019 %, n=6; p=0.0651. Mann-Whitney, two tailed). **E)** Comparison of field EPSPs during the 5 minutes (=15 recording) of baseline pre tetanic stimuli, the first five minutes post tetanic stimuli and the last five minutes post tetanic stimuli. The results are shown for each sequence as percentage of baseline. There is a significant increase in fEPSP (averaged over the first five minutes responses post tetanic stimuli=15 recording) compare to the baseline in the Camk2αCre-WT mice but no difference is observed in the Camk2αCre-cKO mice (Camk2αCre-WT: Baseline fEPSPs=101.78±1.60 %, First 5 minutes fEPSPs=135.06±15.64 %, n=6; p=0.026; Camk2αCre-cKO: Baseline fEPSPs=98.78±2.06 %, First 5 minutes fEPSPs=98,83±2,86 %, n=6; p=0.8182. Mann-Whitney, two tailed). For the Camk2αCre-WT, the response was maintained for over an hour, as the fEPSP during the last 5 minutes after the tetanic stimuli were still significantly higher than the baseline (Baseline fEPSPs=101.78±1.60 %, Last 5 minutes fEPSPs=151.35±11.34 % n=6; p=0.0022, Mann-Whitney, two tailed). (* - p<0.05, ** - p<0.01, *** - p<0.001).

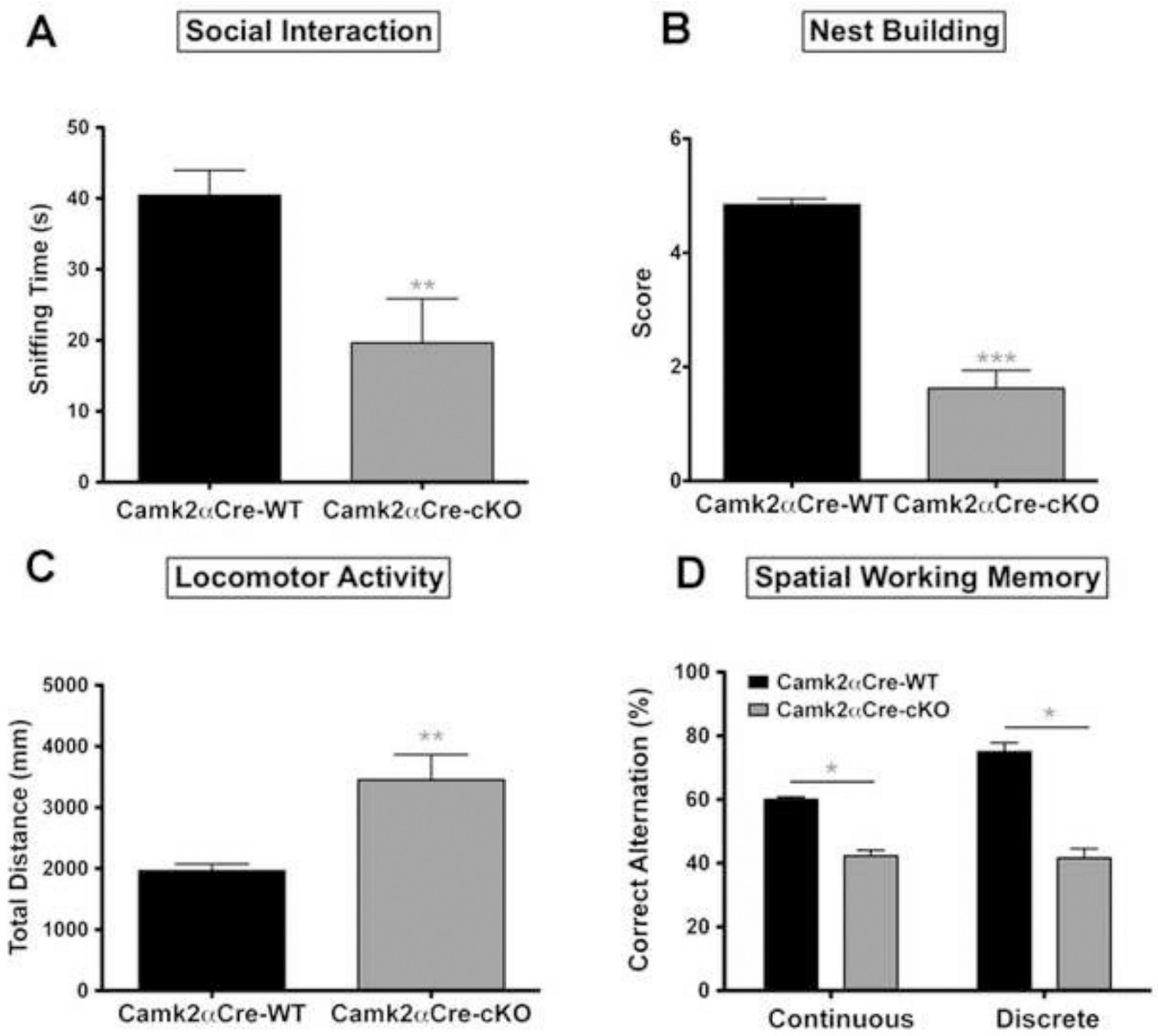

Figure 2. Pyramidal neuron specific NMDA-R1 KO mice show SZ-related behaviors

A) Social interactions were measured in a three-chamber apparatus as previously described. Time spent sniffing the social cylinder (containing the stimulus mouse) is shown. Camk2αCre-cKO mice spent significantly less time interacting with the stimulus mouse than the Camk2αCre-WT mice (Camk2αCre-WT=40.46±3.49 sec, n=17; Camk2αCre-cKO=19.65±6.21 sec, n=16; p=0.008, t=2.92). **B)** Self-care was assessed using a nest building method and the nest quality was quantified from 0 a.u. (poor) to 5 a.u. (best) as previously described. Camk2αCre-cKO mice scored significantly lower for next construction than WT littermates (Camk2αCre-WT=4.85±0.17 a.u., n=13; Camk2αCre-cKO=1.62±0.56 a.u., n=16; p<0.0001, Mann-Whitney, two-tailed). **C)** Locomotor activity was measured in an open field. The Camk2αCre-cKO mice show a significant increase in LMA, as measure by total distance (Camk2αCre-WT=1965±108 cm, n=18; Camk2αCre-

cKO=3454±410 cm, n=18; p=0.0023, t=3.51). **D)** Cognitive function was assessed using the continuous and discrete T-maze. The percentage of correct alternations for each mouse was measured. Camk2αCre-cKO mice show a significant impairment in spatial working memory compared to Camk2αCre-WT mice (Discrete T-maze: Camk2αCre-WT=75±9.70 % of correct alternations, n=12; Camk2αCre-cKO=41.67±10.36 % of correct alternations, n=12; p=0.0284, t=2.34. Continuous T-maze: Camk2αCre-WT=60.04±2.83 % of correct alternations, n=12; and Camk2αCre-cKO=42.36±7.06 %, n=11; p=0.037, t=2.32). Statistical analyses in **(A, C, and D)** were performed using an unpaired, two tailed t-test followed by Welch's post-hoc when appropriate **(A, C and D)**, to correct for unequal variance. Significance after Bonferroni correction requires p=0.0125. (* - $p<0.05$, ** - $p<0.01$, *** - $p<0.001$).

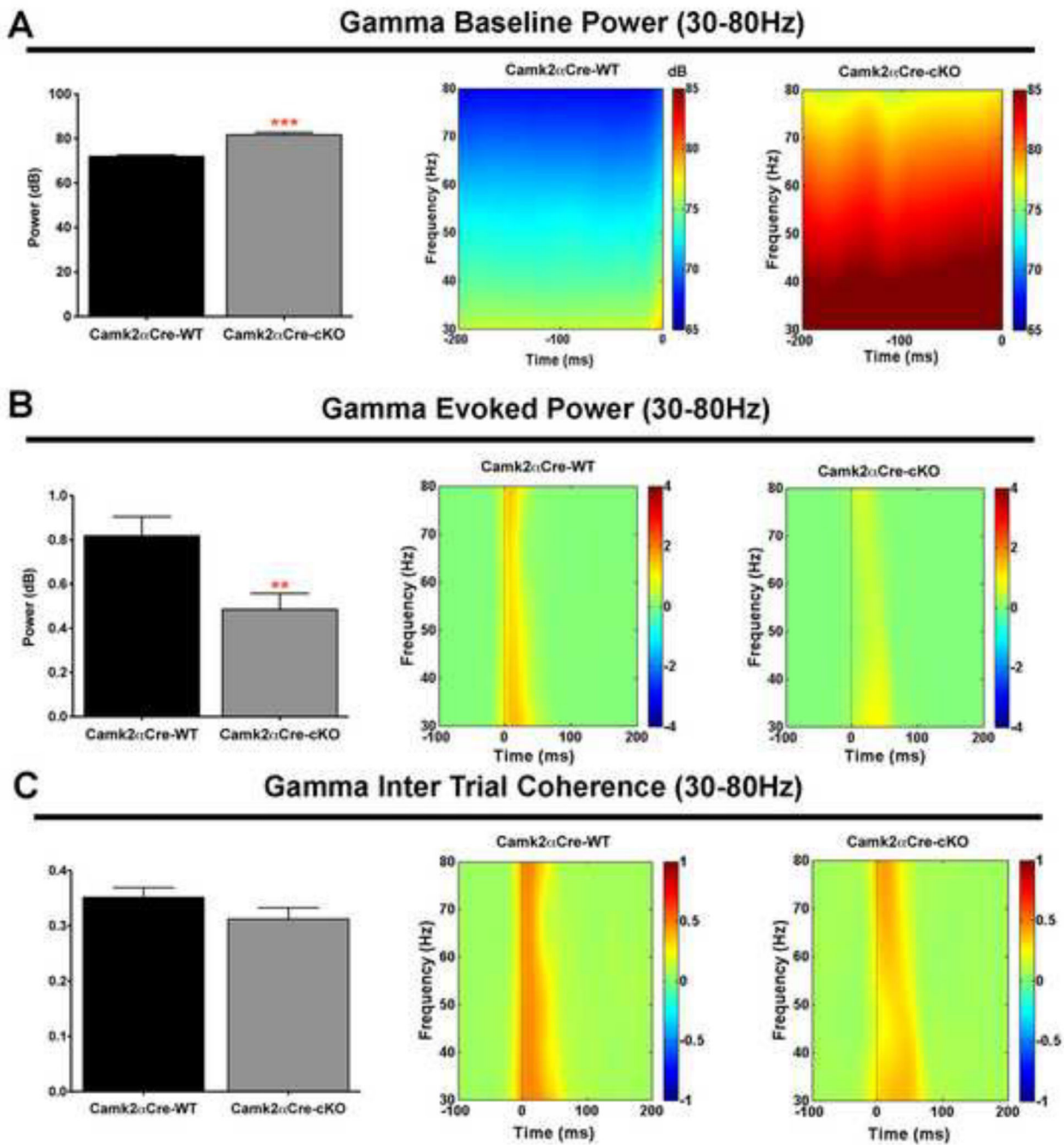

Figure 3. Gamma band oscillatory activity is disrupted in pyramidal neuron specific NMDA-R1 KO mice

A) Camk2αCre-cKO mice show a significant increase in baseline gamma power compared to the wild type mice recorded from −200ms to 0ms before the stimulus (Camk2αCre-WT=71.92±0.51 dB, n=17; Camk2αCre-cKO=81.66±1.10 dB, n=16; $p<0.001$, $t=8.02$). Result is illustrated on the time-frequency decomposition map shown at the right of the histogram. **B)** Evoked gamma power, measured within 50ms following the stimulus, was decreased in the Camk2αCre-cKO compare to the Camk2αCre-WT mice (Camk2αCre-

WT=0.82±0.09 dB, n=17; Camk2αCre-cKO=0.48±0.07 dB, n=16; p=0.0062, t=2.95). Result is illustrated on the time-frequency decomposition map shown at the right of the histogram. **C)** The inter-trial coherence (ITC) representing the level of synchrony of oscillatory activity between trials at gamma band frequency was qualitatively, but not significantly decreased in Camk2αCre-cKO mice (Camk2αCre-WT=0.35±0.02, n=17; Camk2αCre-cKO=0.31±0.02, n=16; p=0.156, t=1.46). ITC is measured in degrees of phase coherence ranging from 0 = no coherence to 1 = perfect coherence(111). Result is illustrated on the time-frequency decomposition map shown at the right of the histogram. Statistical analysis in **(A, B and C)** were performed using an unpaired two tailed t-test followed by Welch's post-hoc when appropriate **(A)**, to correct for unequal variance. Significance after Bonferroni correction requires p=0.006. (* - $p<0.05$, ** - $p<0.01$, *** - $p<0.001$).

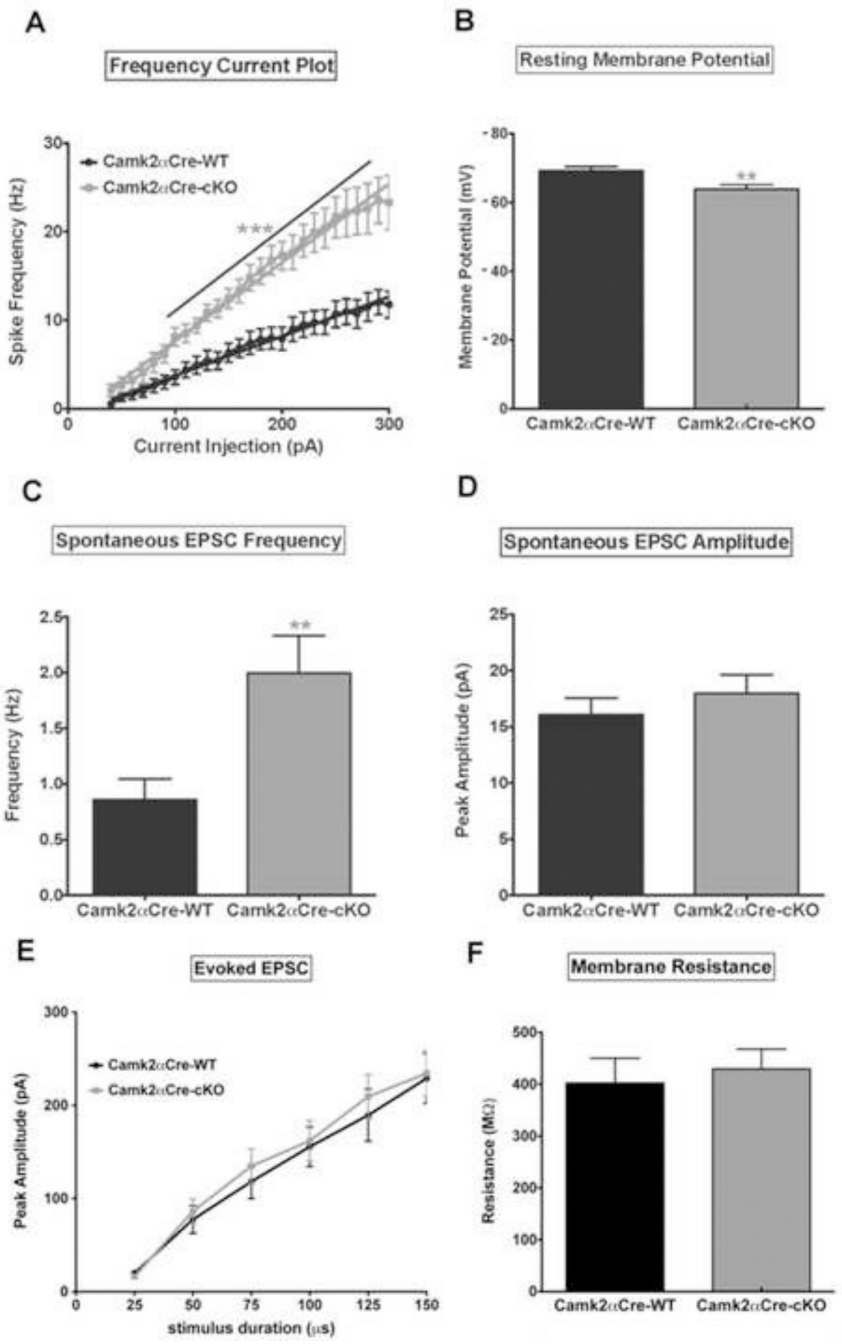

Figure 4. Loss of NMDA-R1 in pyramidal neurons leads to an increase in pyramidal cell excitability

Patch clamp was used to determine the electrophysiological cellular properties of pyramidal neurons. **A)** Frequency-current (F–I) plot show an increase in spike frequency as a function of increasing current injection in both groups of mice. Note the significantly higher rate of spike frequency firing in Camk2αCre-cKO mice compared to Camk2αCre-WT mice (n=13 for each group, $p<0.001$, Sum-of-squares=8653, F=296.5. Two-way ANOVA with Bonferroni post-hoc). **B)** Pyramidal neurons from Camk2αCre-cKO mice are more depolarized at rest compared to the Camk2αCre-WT mice (Camk2αCre-WT=−69.21±1.24

mV, n=13; Camk2αCre-cKO=−63.88±1.31 mV, n=13; p=0.007, t=2.95). **C, D)** Pyramidal neuron spontaneous EPSC frequency **(C)** and peak amplitude **(D)** are both increased in Camk2αCre-cKO mice but the increase reached significance only for frequency (Frequency: Camk2αCre-WT=0.86±0.18 Hz, n=14; Camk2αCre-cKO=2.00±0.33 Hz, n=15; p=0.007, t=2.97. Peak amplitude: Camk2αCre-WT=16.08±1.48 pA, n=13; Camk2αCre-cKO=17.95±1.69 pA, n=15; p=0.418, t=0.823). **E)** There was no significant difference for peak amplitude of evoked EPSCs between the 2 groups (p=0.445, Sum-of-squares=1298, F=0.592. Two-way ANOVA with Bonferroni post-hoc). **F)** The Resistance did not differ significantly between the two groups of mice (Camk2αCre-WT=402.3 ± 47.99 n=14; Camk2αCre-cKO=429.6 ± 38.20 n=19; p=0.660; t=0.444). Statistical analysis in **(B, C, D and F)** were performed using an unpaired two tailed t-test followed by Welch's post-hoc when appropriate **(C)** to correct for unequal variance. Significance after Bonferroni correction requires p=0.007. (* - p<0.05, ** - p<0.01, *** - p<0.001).

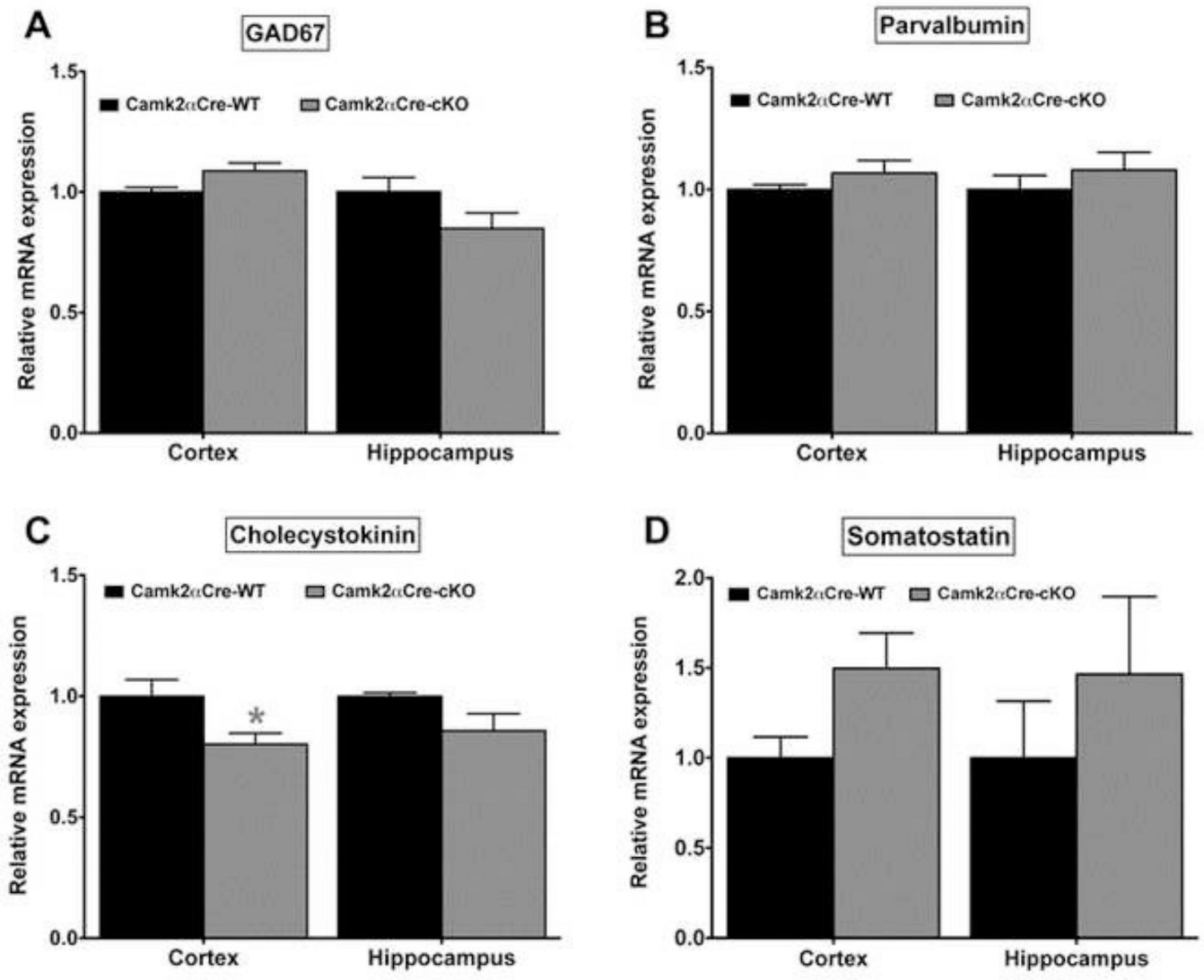

Figure 5. GABAergic interneurons alteration in the cortex and hippocampus of Camk2αCre-cKO mice

A) The expression of GAD67 mRNA was not significantly changed in the Camk2αCre-cKO mice (**Cortex**: Camk2αCre-WT=1.0±0.02, n=7; Camk2αCre-cKO=1.09±0.03, n=7; p=0.053. **Hippocampus**: Camk2αCre-WT=1.0±0.06, n=7; Camk2αCre-cKO=0.85±0.06, n=7; p=0.165) **B)** The expression of PV mRNA was unchanged in the Camk2αCre-cKO mice (**Cortex**: Camk2αCre-WT=1.01±0.07, n=7; Camk2αCrecKO= 1.14±0.06, n=7; p=0.421. **Hippocampus**: Camk2αCre-WT=1.0±0.06, n=7; Camk2αCre-cKO=1.23±0.12, n=7; p=0.548). **C)** The expression of CCK mRNA was decreased in both cortex and hippocampus, the difference being significant only in the cortex (**Cortex**: Camk2αCre-WT=1.0±0.06, n=7; Camk2αCre-cKO=0.81±0.04, n=7; p=0.017. **Hippocampus**: Camk2αCre-WT=1.0±0.04, n=7; Camk2αCre-cKO=0.88±0.05, n=7; p=0.151). **D)** somatostatin (**Cortex**: Camk2αCre-WT=1.0±0.08, n=7; Camk2αCre-cKO=1.42±0.16, n=7; p=0.056. **Hippocampus**: Camk2αCre-WT=1.0±0.22, n=7; Camk2αCre-cKO=1.47±0.32,

n=7; p=0.259). Mann-Whitney, two tailed, all samples were run in duplicate. Significance after Bonferroni correction requires p=0.012 (* - p<0.05, ** - p<0.01, *** - p<0.001).